THE ANTI-ARRHYTHMIC EFFECTS OF CONSTANT DIASTOLIC INTERVAL PACING IN A NUMERICAL MODEL OF A CANINE CARDIAC VENTRICULAR FIBER

A THESIS
SUBMITTED TO THE FACULTY OF
UNIVERSITY OF MINNESOTA
BY

CHRISTOPHER DANIEL JOHNSON

IN PARTIAL FULFILLMENT OF THE REQUIREMENTS
FOR THE DEGREE OF
MASTER OF SCIENCE

ALENA TALKACHOVA

June 2016

Acknowledgements

This project would not have been possible without the help of numerous individuals including my advisor Dr. Alena Talkachova who guided me throughout the process and shaped me into the researcher I am today. Many thanks as well to my lab: Elizabeth Annoni, Steven Lee, Kanchan Kulkarni, and Dr. Sharon Zlochiver who all assisted in the review and troubleshooting of this project. A special thanks to Dr. Stephen McIntyre for allowing me to continue his work and his assistance in the project.

A special thanks also to my coaches at the University of Minnesota: Kelly Kremer, Gideon Louw, Steve Miller, Ryan Purdy, Terry Ganley, and the entire athletic department and support staff, for being so accommodating with my academic pursuits. Another special thanks to my former coaches Bill Tramel and Denis Dale for recruiting me and giving me a shot. A thank you to the Big Ten Conference for awarding me with the post graduate scholarship that supported me partially financially during this pursuit. Also thank you to all my teammates throughout the years especially CJ Smith, Garin Marlow, Andrew Hartbarger, Brian Gorman, Matt Barnard, Mike Nunan and the other members of the Perch, for all the long nights joining me to study. Thank you to the Fab Five (Reid, Paul, Aidan, and Ben) for always being supportive and keeping me encouraged. And thank you Haley Spencer and Karlee Bispo for helping proof read.

Finally, thanks to my family for the moral and financial support throughout my collegiate career; Mom, Dad, Philip, Oma und Opa, Grandma and Grandpa, Tante Marielle und Onkel Franz, and all of my extended family on the Johnson and Manzenrieder sides.

Dedication

To Mama, Dad, Philip and all my family

Abstract

Beat to beat changes in action potential duration (APD) are known as alternans. Alternans are precursors for cardiac arrhythmias that may lead to heart failure and sudden cardiac death. Sudden cardiac death makes up 15-20% of all deaths annually in the United States (Deo, [28]). Alternans are known to form in association with periodic pacing protocol, during which the basic cycle length (BCL) is held constant. Periodic pacing incorporates feedback from the previous action potential, allowing for the formation of alternans. Constant diastolic interval (DI) pacing relies on the elimination of feedback within the system, and through the elimination causes the suppression of alternans. It has previously been shown that alternans suppression within a single cell model is possible (McIntyre, [22]).

This research focuses on the presence and behavior of alternans in a 150 cell (1.5cm) and a 300 cell (3cm) cable during constant BCL and constant DI pacing.

Alternans did appear for constant DI pacing for DI values lower than 20ms, representing a non-physiological range. However, we found that alternans could be controlled using a constant DI pacing protocol for both a short and long cable when using physiological ranges for DI, above 30ms.

Table of Contents

List of Figures

CHAPTER 1

INTRODUCTION

1.1 Cardiac physiology

The heart is a complex organ that is comprised of an intricate electrical signaling pathway synchronized with mechanical activity. It supplies the body with nutrients for survival. A contraction is initiated by the sinoatrial (SA) node, the main pacemaker and starting point of the electrical cascade throughout the atria and ventricle (Robinson, [1]). The pacemaker cells in the center of the SA node provide the origin of the cardiac electrical impulses, called action potentials, that propagate throughout the heart. Cardiac action potentials are created by the combination of various ionic currents including 2 delayed rectifying potassium currents (I_{Kr} and I_{Ks}), a L-type and T-type calcium current ($I_{Ca,L}$ and $I_{Ca,T}$), hyperpolatization-activated cation current (I_f) as well as multiple others (Vinogradova, [2]).

Once the action potential has been initiated, it travels away from the SA node to the AV node and through the Purkinje fibers to the ventricles by utilizing an inward sodium current (I_{Na}) to depolarize the membrane and then the inward L-type calcium current ($I_{Ca,L}$) to repolarize the membrane (Grant [3]) (Figure 1). The action potential (AP) propagates from cell to cell and throughout the heart by ionic channels and ionic gradients that assist the voltage to travel in one direction toward the ventricles (Grant, [3]). Depolarization of the heart correlates with the contraction of the heart muscle,

while repolarization corresponds with the relaxation phase. The dynamics of the varying electrically coupled components are shown in Figure 1, where each part of the activation series is shown with its corresponding unique AP (Figure 1).

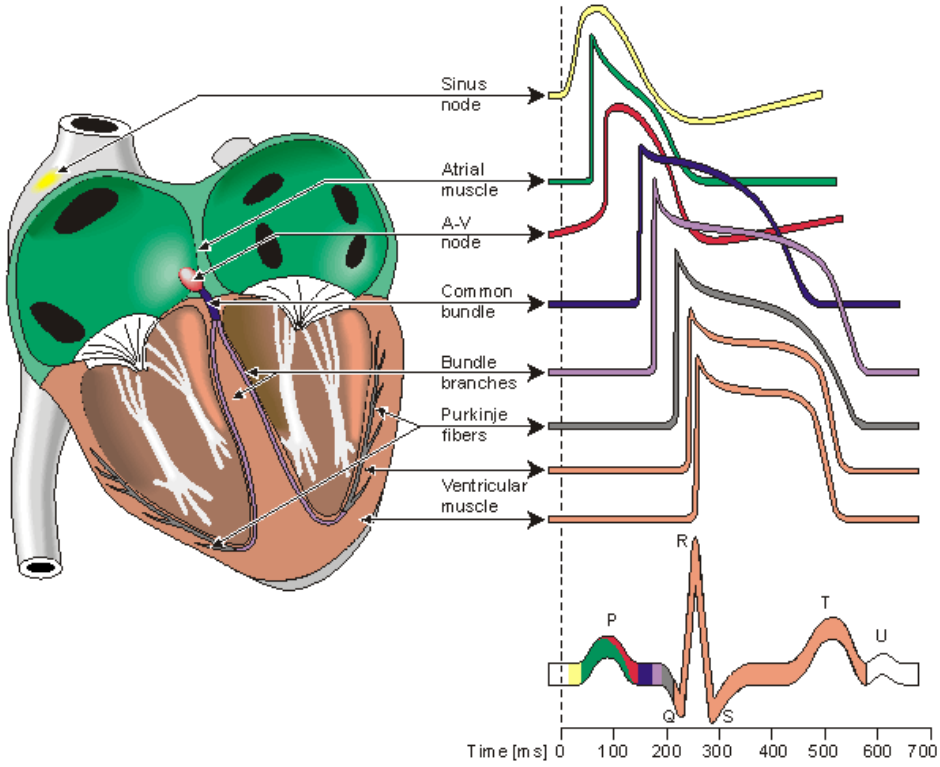

Figure 1 - Whole heart with activation series and corresponding action potentials [35].

To cycle through over 100,000 contractions a day the heart relies on excitation-contraction (EC) coupling (Pinnel [4]). EC coupling is the mechanism that couples the opening of voltage-gated calcium channels, activated by the propagating action potential, to the contraction of the muscle (Hopkins, [5]). The contraction of the muscle is caused by a calcium induced calcium release from the sarcoplasmic reticulum (SR) (Hopkins, [5]). EC coupling is crucially involved in the contraction process of a cardiac myocyte (Hopkins [5]).

Cardiac chambers contract and relax to propel blood throughout the body to supply oxygen to all the cells, allowing them to function and maintain homeostasis. Homeostasis within the body is vitally important as without equilibrium the body's processes could collapse and fail (Kolwicz, [6]). Homeostasis is maintained in many systems; mechanically, the heart maintains oxygen and nutrient homeostasis within the peripheral cells. To do this, the myocardial surface needs to remain homeostatically balanced in respect to ion distribution (Schmidt, [7]). If the balance of ions and the potential gradients is disturbed, unexcitable regions may be created (Barth, [8]). Areas of unexcitable tissue could also be caused by scarring or other damage caused by either previous cardiac episodes or ionic imbalance (Rubart, [9]). Areas of imbalance or unexcitable tissue may slow down propagation of action potentials. This slowing of a signal may lead to cardiac arrhythmias and in the worst cases, sudden cardiac death (SCD) may occur due to failure of the heart to contract (Rubart, [9]). In these scenarios implantable pacemakers are one of the few viable options to extend life expectancy and improve overall quality of life. (Wood, [22])

1.2 Cardiac arrhythmias

Cardiac arrhythmias occur when the heart contracts out of rhythm and therefore has an abnormal activation sequence (Jaeger, [10]). Each of these occurrences can cause arrhythmias of varying types and severities depending on where the arrhythmia originates as well as what in the activation sequence is affected. The activation

sequence is described as the path of electrical activity stemming from the endocardium to the epicardium (Ramanathan [23]).

Two arrhythmias that relate to the investigation are: ventricular tachycardia (VT) and ventricular fibrillation (VF). VT is an arrhythmia during which the ventricle contracts prematurely, or before the action potential has reached the Purkinje fibers within the conduction system (Stevenson, [13]). VF is associated with a chaotic electrical signal throughout the membrane of the ventricle resulting in the failure to pump blood due to the unsynchronized electrical activity and loss of effective ventricular contraction. All cardiac arrhythmias can be identified on an electro cardio gram (ECG), therefore the symptoms and behaviors are well known. Once a patient has an observable cardiac arrhythmia, implantable cardioverter-defibrillator's (ICD) are often the only option (Wood [22]).

A precursor to cardiac arrhythmias is heart failure (HF), the inability of the heart to pump blood throughout the body (Roger, [29]). In the US 180000 to 450000 people are diagnosed with HF annually (Roger, [29]). Due to this inability to contract, cardiac arrhythmias may arise as the heart is attempting to compensate. HF, if left untreated, may lead to SCD. 15 – 20% of all deaths reported within the US annually are caused by SCD (Deo, [28]). A precursor for cardiac arrhythmias is alternans or beat to beat changes in the length of contractions.

1.3 Alternans

In the ECG, alternans are diagnosed by variations in the T-wave length and shape indicating electrophysiological instability (McIntyre, [22]). These instabilities are a compensation mechanism of the heart to attempt to reach full repolarization and resetting (Rubenstein, [16]). When considering alternans, the first thing that needs to be addressed is the shape of the action potential and variations that may occur due to alternans. As addressed above, action potentials are created by the varying ionic currents flowing in and out of the cardiac myocytes. However, there are multiple characteristic measurements that can be extracted from action potentials to further analyze and evaluate their behavior.

Action potential duration (APD), the first marker that will be analyzed, is a measurement of the length of time the action potential stays elevated above a certain threshold (Figure 2). The threshold is defined by the percent of repolarization of the myocardium. For ventricular myocytes, two common APD values to look at are when the membrane is at 95% of its resting potential (APD_{95}) and similarly when the membrane is at 90% (APD_{90}). These values are also very important when considering alternans as, at 90% repolarization, the membrane has almost reached full repolarization and most likely will reach full repolarization before the beginning of the next action potential.

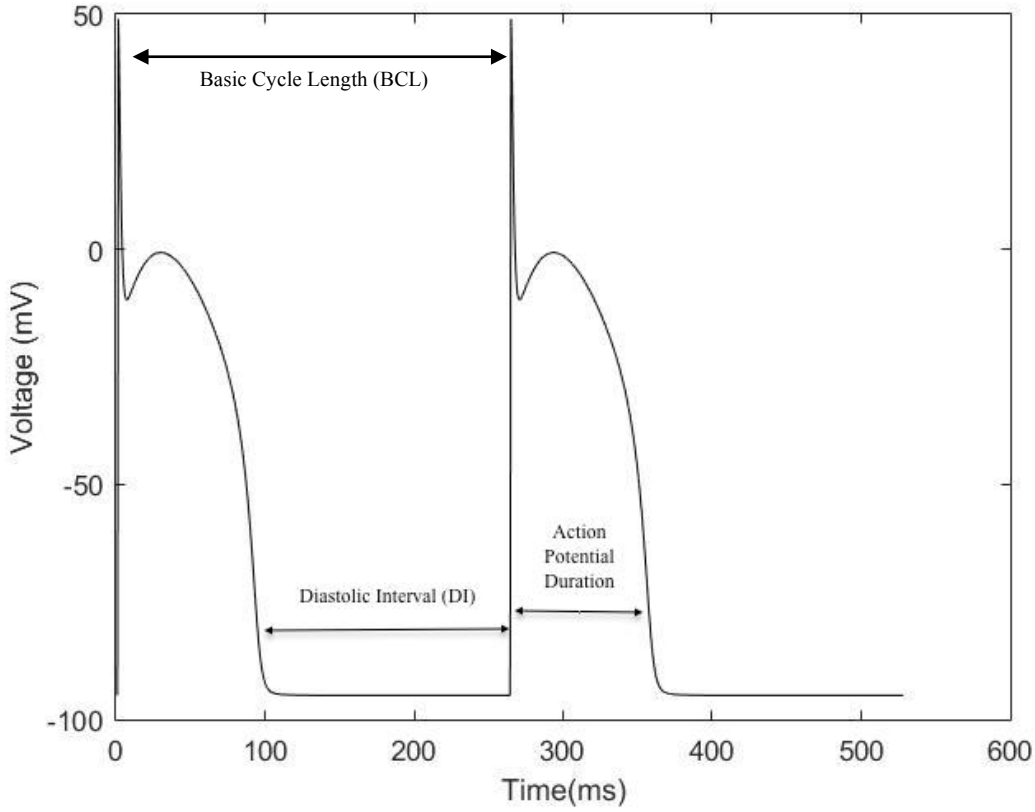

Figure 2 - Voltage trace highlighting Diastolic Interval (DI) length, Action Potential Duration (APD), and Basic Cycle Length (BCL)

The next interval to be more closely discussed is the compliment to the APD, the diastolic interval (DI) (Figure 2). DI refers to the interval during which the potential stays below the percent of repolarization. Mechanically, this is the time in which the ventricles relax and are filled with blood. The DI is important in the context of alternans due to nature of the compensation mechanism in relation to relaxation and repolarization. As the electrical and mechanical components of the heart are linked, a longer DI indicates more filling and a more complete contraction of the heart, creating a longer APD, whereas a shorter DI indicates less blood entering the ventricles resulting in a shorter APD. This interplay between DI and APD is the

underlying reason for the typical shape of alternans of long-short-long APD's and correspondingly the associated DI's being short-long-short (Figure 3). Alternans are defined by a variation of the long-short-long pattern by a difference of more than 5ms (Jordan, [26]). APD and DI combine to make up the basic cycle length (BCL) (Figure 2).

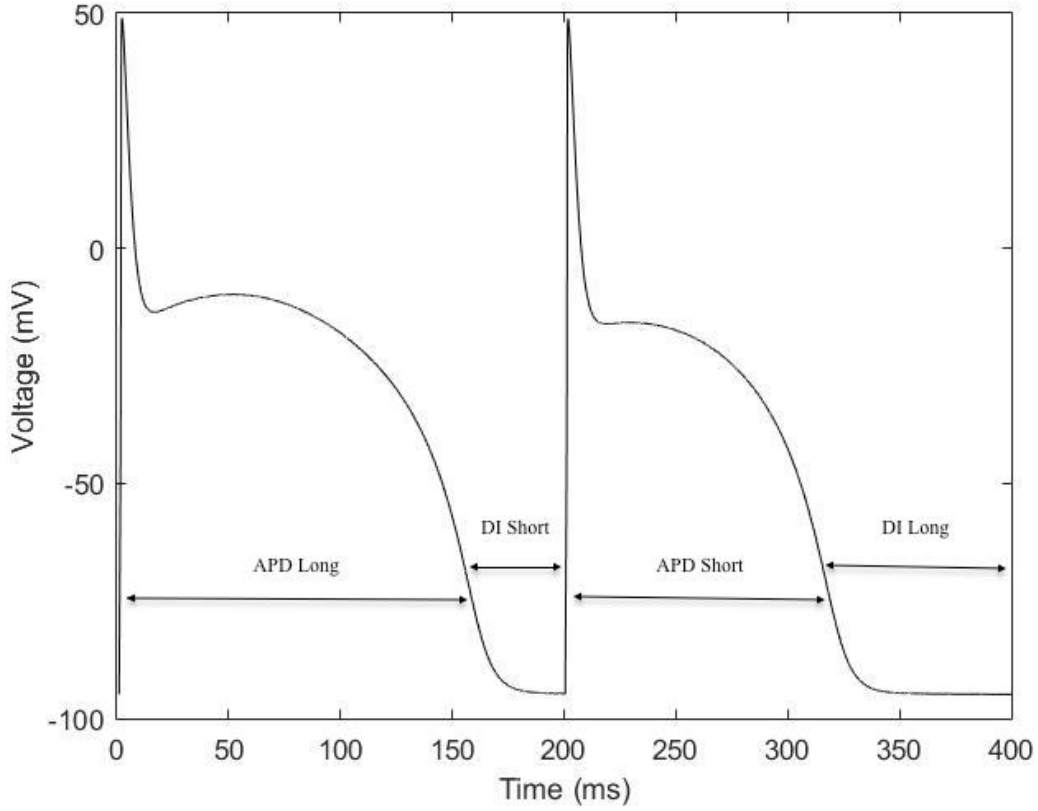

Figure 3 - Voltage traces demonstrating alternans highlighting its characteristic long, short behavior

Alternans description can vary throughout the myocardium depending on location and their relationship of APD to neighboring cells in space. Concordant alternans are often described as alternans that are spatially in phase with the next stimuli (Gaeta [17]). This relationship can be observed in Figure 4, where *a* and *b* represent two

consecutive stimuli. Concordant alternans are spatially shown in the lower part of Figure 4A, where the entire section is one color indicating all APD's are the same length for both stimuli *a* and *b* (Figure 4).

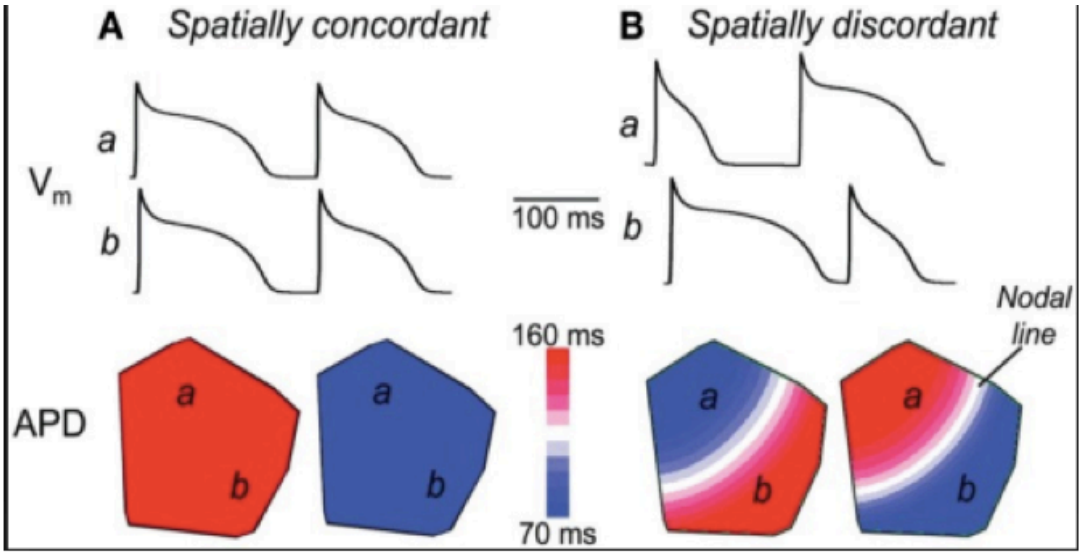

Figure 4 - Voltage traces as well as spatial APD distribution for concordant and discordant alternans for two stimuli (stimuli a and stimuli b) (Gaeta, [17])

The other form of alternans that could appear in space is discordant alternans. Discordant alternans is described when the APD's of two consecutive beats throughout space are different. Figure 4B, shows that stimuli *a* has a short-long pattern, whereas stimuli *b* shows a long-short pattern (Figure 4). Often times when inspecting consecutive beat APD values along the cable they may converge or reverse pattern depending on where spatially they are located in the myocardium (Wei, [18]). These location variances are often referred to as out of phase APD's separated by nodes of convergence; during which, for a short time, the APD's match each other while the previously longer APD shortens and the previously shorter APD elongates.

A nodal line can be identified in Figure 4B, for discordant alternans as the length of APD switch between a short to a long APD (Figure 4).

In a clinical perspective, alternans are precursors for VF due to their formation of electrophysiological instabilities (McIntyre, [22]). The reasoning being is that alternans form a distinct characteristic contraction cycle that attempts to compensate. However, as described above, if alternans are prolonged, the myocardium may show spatially discordant alternans. Discordant alternans are one of the final precursors of VF. As cells no longer contract together the non uniform contractions can create unidirectional block and reentry causing an onset of VF (Pieske, [19]).

1.4 Restitution

Restitution is an inherent property of cardiac myocytes, that relates the APD of a certain activation to it preceding DI. Restitution defines the relationship such that when DI shortens, the following APD also shortens to accommodate (Franz, [40]). The equation describing the relationship between the two measures is

$$APD_{n+1} = f(DI_n) \qquad (1)$$

In equation 1, f represents the restitution curve where the APD is the duration of the (n+1)st APD and the DI corresponds with the current nth stimuli. Figure 5A demonstrates the graph created by equation 1 and the accommodation of the APD in accordance with the previous DI (Figure 5A).

1.5 Feedback

Feedback is defined by the equation based on

$$DI_n = BCL_n - APD_n \qquad (2)$$

Where the BCL is the sum of the current APD and current DI (Figure 2). When the BCL is kept constant at a set value such that $BCL = BCL_n$, there is a partial dependence of DI on the preceding APD, representing the feedback. This partial dependence is demonstrated in Figure 5B, as an inverse relationship between APD and DI, if APD increases in length the DI shortens and vice versa (Figure 5B).

Figure 5 C-E are cobweb diagrams that demonstrate the relationship between DI and APD in the formation of alternans and the role of restitution and feedback (Figure 5). Each graph for Figure 5 C-E demonstrates a different behavior of alternans, Figure 5C shows disappearing alternans as the APD and DI approach the intersection point on the graph. Figure 5D shows stable alternans maintaining a consistent pattern of

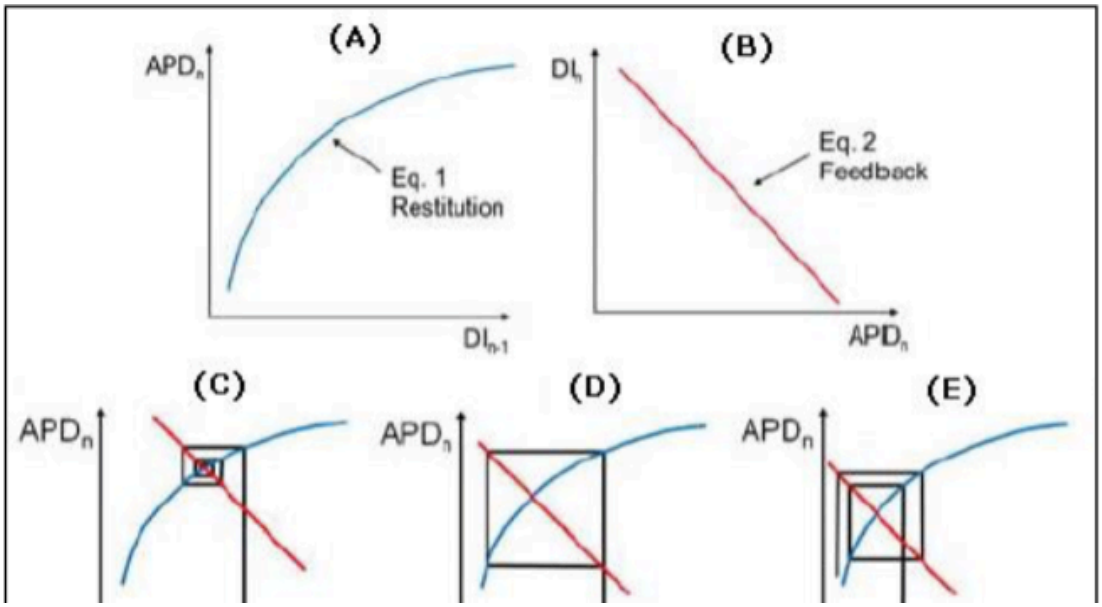

Figure 5 - 5A shows the restitution graph, 5B shows, the feedback graph 5C-E show the cobweb diagrams of alternans formation with feedback in the system

APD and DI values. Figure 5E shows diverging alternans where the APD and DI fluctuations are increasing. The creation of diverging, converging, and stable alternans can also be correlated to the slope of the restitution curve dependent on where the feedback curve intersects the restitution curve. Figure 5 C demonstrates that when the slope of restitution is less than 1 when the feedback curve intersects it the alternans formed are converging. Similarly, in Figure 5 D the feedback curve intersects the restitution curve at a slope exactly at 1, corresponding with stable alternans. Finally Figure 5E show that when the slope of restitution is greater than 1, alternans will diverge (Figure 5).

1.6 Pacing

Proarrhythmic describes a pacing protocol that results in the formation of arrhythmias, often identified by the formation of alternans. In contrast antiarrhythmic pacing protocols result in no arrhythmias and no formation of alternans.

Periodic pacing (applying a stimulus after a constant BCL ($BCL_n = BCL$)), incorporates feedback as described in equation 2, and has been shown to be proarrhythmic (Pinski,[11]). Figure 6 demonstrates the basic nature of periodic pacing where a stimulus is applied after set BCL, indicated by the green double headed arrows (Figure 6). Periodic pacing, is the traditional method used in implantable pacemakers that are usually implanted in patients suffering or at high risk of heart failure (Pinski, [11]). For these patients, the importance of generating a stimulus is more important than the side effects that periodic pacing may cause, such as alternans

leading to arrhythmias. In periodic pacing, proarrhythmic effects can be seen when stimuli are applied in quick succession (Koneru, [12]). The reasoning is that when periodic pacing is applied for multiple successive beats, the pacing may cause an arrhythmia such as VT or VF, during which the heart does not have enough time to naturally reset and relax and becomes overloaded with stimuli. This overstimulation causes premature beats in the ventricle leading first to re-entrant VT and if continued, the heart may fall into VF, during which no contraction occurs (Samie, [14]).

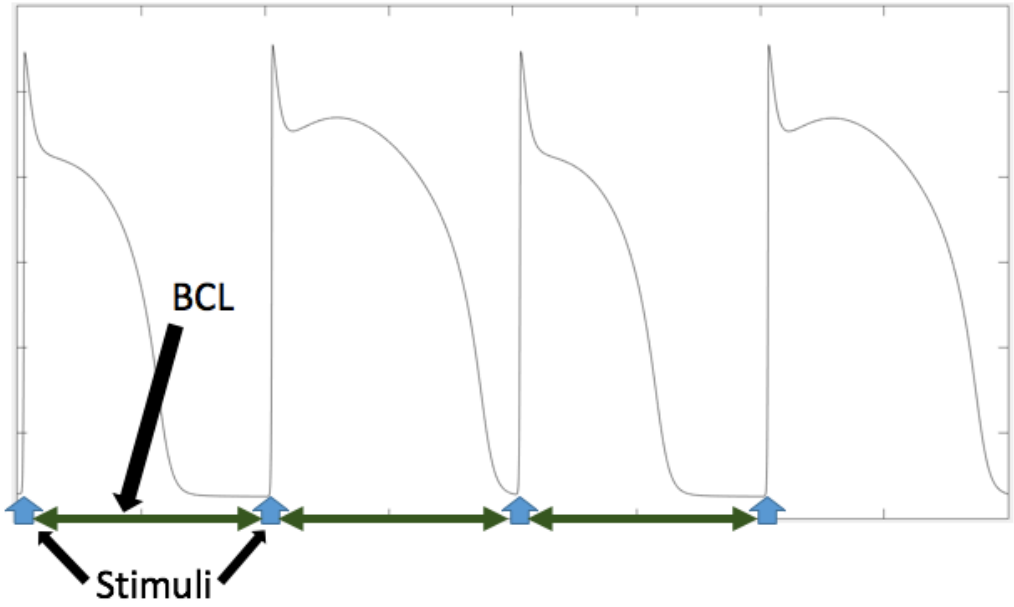

Figure 6 – Voltage trace for periodic pacing with indicated BCL interval (Green double headed arrow) and stimuli application (Blue arrow)

Within a protocol that has no feedback, equation 2 no longer hold, so DI is independent of APD. By eliminating the dependence on feedback, alternans formation should be suppressed due to the creation of a mechanism that is not dependent on the restitution curve.

Constant DI pacing eliminates feedback by allowing a predetermined time to pass after repolarization has been achieved. This is in order to allow the membrane to rest and excitability to recover. Figure 7 shows the constant DI interval, indicated by the green double headed arrows, and the following stimuli applied after the interval passed (Figure 7). The removal of feedback within the loop, separates the

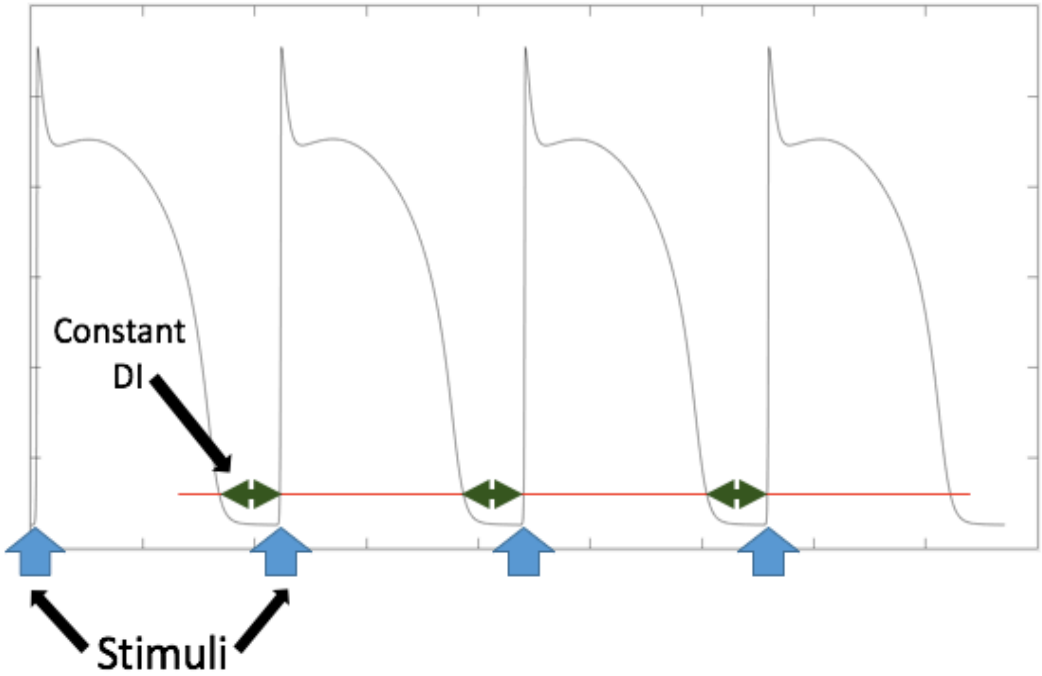

Figure 7 – Voltage trace for constant DI pacing, constant DI (Green double headed arrows) shown and stimuli application (Blue arrow)

dependence on the preceding action potential. This also minimizes the formation of alternans, as the heart does not need to compromise and attempt to create shorter APD's to allow for repolarization and resetting of the membrane gradients to resting levels. Therefore, through the elimination of feedback and manually adjusting the DI, alternans formation should be able to be suppressed and controlled.

1.7 Previous findings

Various research has been conducted, beginning in the early 2000's to the present day, into the area of alternans suppression and control using constant DI pacing. Each approach varies in how constant DI was applied and interpreted to optimize control.

The first findings by Jordan et al. in 2004, showed that using their adaptive diastolic interval pacing protocol applied to a Fox canine model, alternans formation could be controlled in a short cable. Adaptive diastolic interval pacing protocol is a protocol described by the equation,

$$DI_{n+1} = DI_n + \alpha[BCL^* - BCL_n] \qquad (3)$$

Where alpha (α) is a constant between 0 and 1, and BCL* is the final BCL attempting to be reached. This protocol set out to to slowly increase the DI_{n+1} until it matched the DI of BCL* during which, when paced periodically alternans formed. As the protocol still included BCL feedback was still present. Using an adaptive diastolic interval pacing protocol, alternans formation could be controlled for cables less than 0.5 cm and discordant alternans could be controlled for cables less than 3 cm in length. They found that when applying their adaptive protocol, of controlling the DI, to the action potentials of the Purkinje fibers, they were able to immediately see an elimination of alternans, indicating that their DI pacing has an immediate effect at the pacing site (Jordan, [26]).

The next major investigation of constant DI protocol pacing was performed by Wu et al., in 2006. This group found that when a constant DI pacing paradigm is applied to five adult canines tissue samples, alternans could neither be suppressed or controlled (Wu, [27]). Findings did indicate that using constant DI pacing, changed the pattern of alternans from those seen in constant BCL pacing (Wu, [27]). This pattern was that usually, as described above, long DI's are followed by long APD's, and short DI's are followed by short APD's. Wu et al. however, found holding the DI constant created a pattern of constant DI followed by long APD, and constant DI followed by short APD, indicating an adaptive alternans pattern (Wu, [27]).

Lastly, numerical modeling performed in our lab, in 2014, using a feedback elimination approach, showed that alternans can be controlled for various DI's in a single cell model. McIntyre et al. discovered that using a constant DI pacing protocol on a Fox model single cell of the ventricle alternans could be eliminated, by stepping the diastolic interval down beginning at 264ms until 35ms in varying steps sizes smaller than 5ms (McIntyre, [15]).

These three publications show the various conflicting findings concerning the control or suppression of alternans. Jordan et al. showed that alternans could be controlled using an adaptive constant DI pacing protocol. In contrast, Wu found in actual tissue alternans could not be controlled at all (Jordan [26], Wu [27]). Therefore, this study uses the pacing protocol from McIntyre et al. in a cable model in an attempt to investigate if alternans can be controlled for a longer cable or prevented all together (McIntyre, [15]).

CHAPTER 2

METHODOLOGY

2.1 Model

The basis of the model used for this work was the Fox model (Fox, [20]). The model was chosen for several reasons: the model takes into account all the major ion currents present within the myocardium; is able to implement periodic pacing; and finally, the model has the ability to form alternans (Fox, [20]). These three characteristics allow the model to be viable, realistic, and physiologically comparable to real tissue.

The membrane voltage can be calculated by applying current conservation principles on the classical parallel conductor model (Jordan, [26]).

$$\frac{\partial V}{\partial t} = \mathrm{D}\frac{\partial^2 V}{\partial x^2} - \frac{\mathrm{I_{ion}} + \mathrm{I_{stim}}}{\mathrm{C}_m} \tag{4}$$

Equation 4 states that the summation of the capacitive, diffusive and ionic currents must be zero, and is known as the reaction-diffusion equation (Fox, [20]/ Eq 4). The components of this simplified equation are current applied by the stimulation (I_{stim}), current summed by all ion channels crossing the membrane (I_{ion}), the capacitive resistance of the membrane (C_m), the diffusion coefficient for the tissue (D), and the membrane potential (V).

The fluctuations of the ions in relationship to the stimuli allows the code to create the unique ventricular action potential shape associated with a ventricular myocyte. Another key feature of this model is the number of ion channels accounted for, as the more channels accounted for creates a more realistic model.

In addition, the Fox model is versatile with the ability to perform periodic pacing using a set BCL. BCL based pacing is useful to this investigation, as this is the primary method used within pacemakers (Topilski, [24]). Therefore, to create a realistic model to study the pacing of the myocardium with a pacemaker, a consideration for periodic pacing needs to be included.

Lastly, the third characteristic of the Fox model is its ability to create alternans. This is the key reason for our study using the Fox model, as we are investigating the effects of various pacing protocols in respect to alternans formation or suppression. Alternans formation is a natural occurrence within the myocardium therefore, the ability of the program to produce alternans adds to its viability.

The alternans formation of the model is supported by incorporating feedback, to allow the ion distributions across the membrane to not reset but rather draw upon the previous cell's values. This recollection allows the cable to have the ability for feedback, based on the previous APD, and memory of the ion distribution from the previous stimuli.

In a previous study performed in our lab, researchers adjusted the model to investigate the effects of constant DI pacing for a single cardiac myocyte (McIntyre,

[15]). This was done by applying a stimulus after a predetermined DI had occurred. For a constant DI approach, APD's must be monitored to start the DI time interval at the appropriate instant.

2.2 Single Cell Confirmation

To begin the study, the findings of previous researchers in our lab had to be confirmed: 1) that alternans could form during periodic pacing; and 2) that they were able to be suppressed when applying a constant DI pacing protocol in a single cell (McIntyre, [15]).

For the constant BCL testing no issues occurred in the single cell model and alternans formation did occur at a BCL around 200ms. The precise value can only be estimated due to time step limitations. The onset values are very similar to previously found values (McIntyre, [15]). The constant DI model also worked for the single cell model and alternans prevention was also confirmed.

2.3 Cable model

Once the model for a single cell myocyte had been confirmed, the length of the cable was extended to 150 cells or roughly 1.5cm. Each cell has its own unique system of equation associated with its location within the cable and stimulus experienced. Using the Crank-Nicolson method, all the equations for each cell can be combined and made dependent on each other, in particular the adjacent neighbors. The Crank-Nicolson method results in a second-order convergence in time (Kleefeld,

[25]). Convergence in time is beneficial as the movement of the action potential from cell to cell is time dependent.

Adjusting the constant BCL code encountered no issues. This was confirmed by the voltage traces of the action potentials shifting farther away from the original stimulation spot when plotted (Figure 8). This indicated a lag time between the upstroke of cell 15 to cell 115 illustrated in Figure 8, demonstrating a conduction velocity of .34 m/s (Figure 8). Conduction velocity is the speed at which a action potential travels down the cable. Besides the length of the cable, no changes were made to the model.

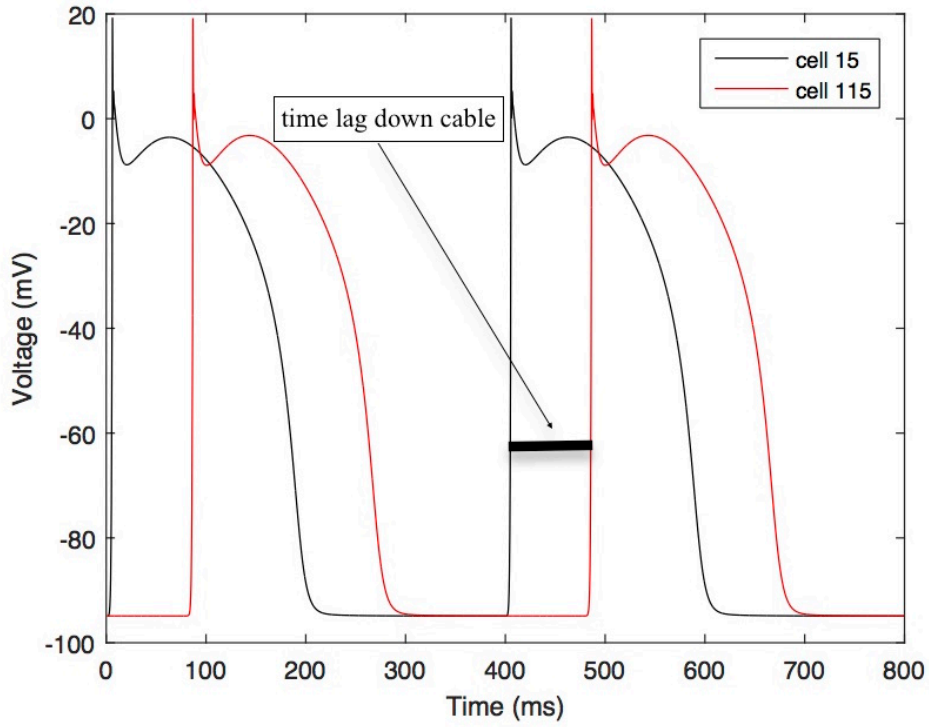

Figure 8 - cell 15 and 115 for periodic pacing at 400ms showing time lag down length of cable

2.4 Adjusting for constant DI

After the conversion of the single cell model to the cable model, the next adaption of the code needed to be made to the pacing protocol. The code began as a constant BCL pacing protocol, therefore accommodations needed to be made for a constant DI protocol. This was done by storing the current stimuli's APD, by recording the moment when 95% repolarization was reached. Following a predetermined DI interval, based on previous experiments on a single cell model, the next stimulus was applied by the model (McIntyre, [15]).

2.5 Testing parameters

The testing parameters for the constant BCL protocol were twofold one for a shorter cable of 150 cells (1.5cm) and the second for a longer cable of 400 cells (4cm). For the shorter cable a down sweep pacing protocol was used beginning at a BCL of 250ms and stepping down by 10ms until the final BCL value of 100ms was reached. At each BCL the cable was exposed to 70 stimuli in order to ensure steady state was reached. For the longer cable no down sweep protocol was used instead the cable was just exposed to BCL of 200ms for 70 stimuli.

Following the constant BCL protocol, constant DI code needed to be adjusted with the correct parameters. The parameters were similar to the constant BCL in that, two cables a shorter 150 cell (1.5 cm) and a longer 300 cell (3cm) were selected. A 300 cell cable was selected instead of a 400 cell cable similar to the constant BCL protocol, because for the longer cable under constant BCL pacing a node formed

around cell 200 within the cable. A node indicated an area of interest if constant DI pacing could still hold, therefore a cable only long enough to include the node position was selected. A 300 cell cable also saved on computation run time. The shorter cable again was exposed to a down sweep protocol, beginning at a constant DI of 200ms and taking two 50ms steps initially until 100ms was reached. The final seven steps were done in 10ms steps, each DI value was paced at 50 stimuli. Only 50 stimuli were used in order to shorten run time, it was discovered that the code had reached stable state after 5 stimuli therefore 50 stimuli were sufficient.

The final protocol applied was a combined protocol of both constant BCL and constant DI. Two cable length were again selected, a shorter 50 cell (.5 cm) and a longer 100 cell (1cm). The shorter cable was first paced under a constant BCL protocol at 200ms for 20 stimuli and then paced under a constant DI protocol at 40ms for 20 stimuli. The longer cable was initially paced for 50 stimuli at a constant BCL of 200ms and then paced for 50 stimuli at a constant DI of 40ms.

2.6 Analysis

The membrane voltage tracings for each cell were analyzed at each stimulus. These voltages were used to determine the APD and DI interval for each pacing protocol. Using MATLAB, voltage tracing graphs provide a visual of the action potential for each stimulus in each cell (Figure 2). After separating the voltage traces, values were used to calculate APD_{90}, to plot restitution plots for both pacing paradigms.

CHAPTER 3

RESULTS

3.1 Constant basic cycle length pacing

During constant BCL pacing, or periodic pacing there are two patterns that can occur. These patterns are defined by the length of the BCL at which the cable is paced, and if this length corresponds with alternans formation. No alternans formed in higher BCL's seen in Figure 5, where the first four dots align perfectly. This relationship of perfect alignment is seen in Figure 9, where the APD values for the last odd and even beat (69 and 70) are plotted along the length of the cable (Figure 9).

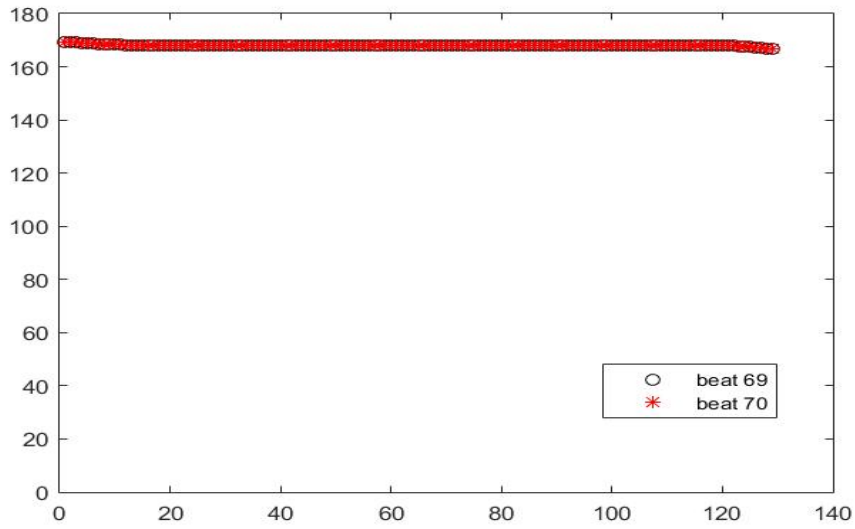

Figure 9 – Progression of APD values down the length of the cable at a BCL of 250ms

Alternans formation is consistent throughout the cable at lower BCLs, observed by the distinct separation seen in the APDs along the cable in Figure 10 (Figure 10). The two lines represent the presence of alternans, exact onset of formation can be

found in the bifurcation curve in Figure 11 (Figure 11). From the restitution curve it can be deduced that alternans begin within the cable around a BCL value of 220ms (Figure 11). To produce Figure 10, the APD values were plotted along a 150 cell cable for a stimulation protocol of 200 ms for the last odd and even beat, beat 69 and

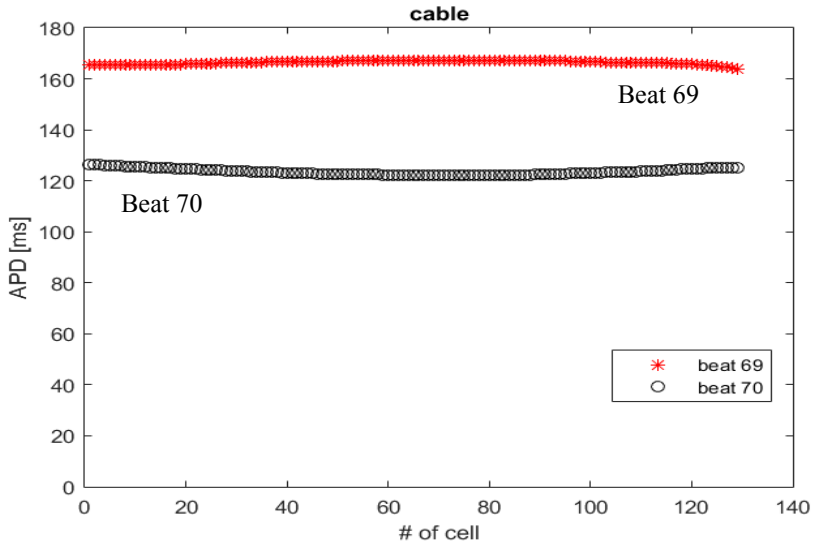

Figure 10 - Shows the progression of APD's along 150 cell (1.5cm) cable (first and last ten cells omitted to avoid edge effects) for the last two stimuli tested (69 and 70) at a BCL of 200ms

70 (Figure 10). This distinction can be observed, that initially at the first cell the difference between beat 69th and 70th beat is 37ms. Throughout the cable this difference increases up to about 45 ms around cell 90. Figure 10 shows the cable with the first and last ten cells removed to eliminate edge effects. The first ten cells were removed in order to avoid stimulation interferences as the stimuli was applied to these cells. The last two beats were chosen due to the nature of alternans to form on odd and even beats and beats 69 and 70 provide a steady state response of the cable.

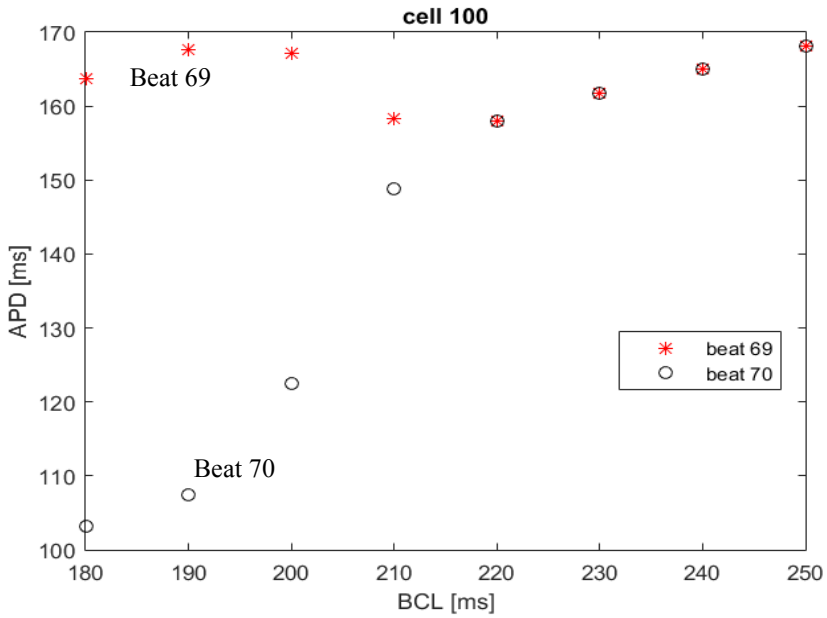

Figure 11 - Shows restitution curve for the 100th cell in the cable, alternans formation can be seen beginning between a BCL of 220ms and 210ms

Figure 11 shows the restitution curve for the 100th cell along the cable (Figure 11). The 100th cell was selected as it lies two thirds of the way down the cable, ensuring steady state as well as minimal border effects. As the BCL lowers the last odd and even beat line up until a BCL value of 220ms, at a BCL value of 210ms the APD values start to diverge. The lower bound of the divergence represents the short beat APD's in contrast to the upper bound being the long beat APD's. Pacing below 180ms revealed 2:1 behavior for 170ms and 160ms followed by conduction block. 2:1 behavior is described as the program only producing one action potential for two stimuli. Conduction block is described as the situation when no response is generated by the program for a stimulus, revealing a flat voltage trace with no action potential.

3.2 Constant diastolic interval pacing

The constant DI protocol results showed that for 150 cell cable alternans did not appear seen in Figure 12, with the 49th and 50th beat being lined up on top of each other along the cable (Figure 12). Beat 49 and 50 were chosen as they were the last odd and even beat in the protocol. The protocol was shortened due to computational time restraints. Once again the first and last ten cells were eliminated to reduce interference of border effects as well as stimulation effects. While the stimulus proceeds down the length of the cable, the value of the APD slowly reduces from

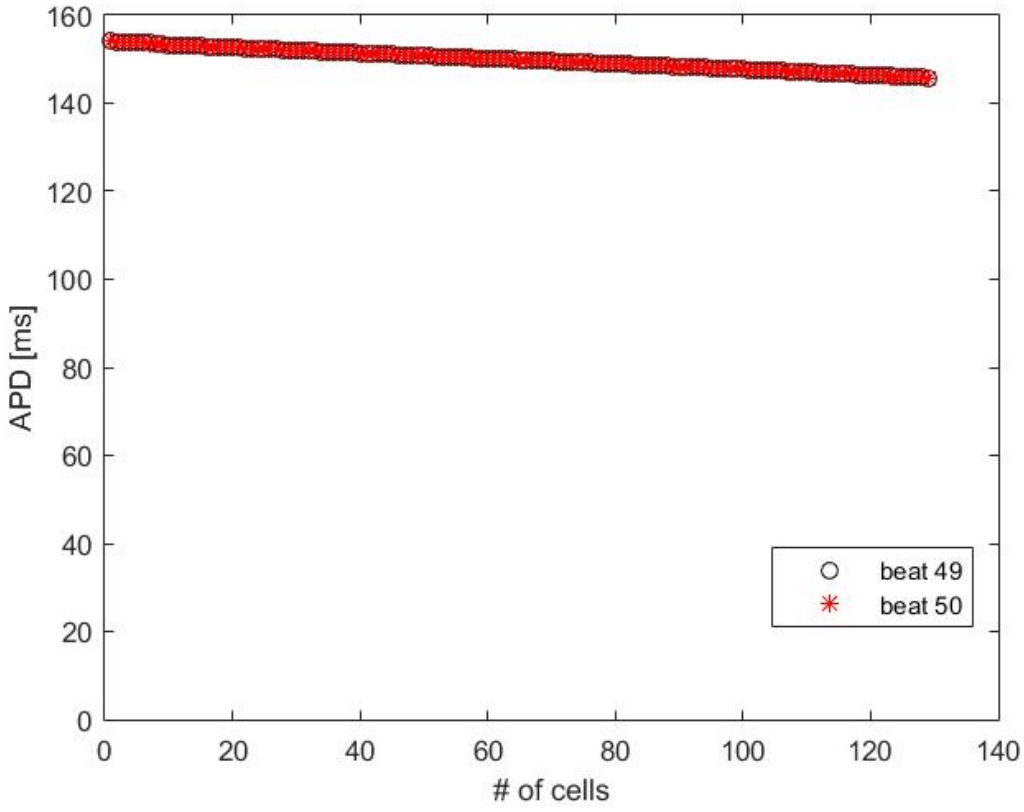

Figure 12 - Shows the progression of APD's along 150 cell (1.5cm) cable for the last two stimuli tested (49 and 50) at a DI held at 55ms, the matching of the black and red indicates no alternans formation throughout the cable first and last 10 cells removed

roughly 154ms at cell 11 the first cell, to 146 at cell 140. The trend of the slow decline in APD values down the cable is identical for both the 49th and 50th beat (Figure 12).

The corresponding restitution curve for the constant DI can be seen in Figure 13 (Figure 13). It shows cell 100 down the cable exhibiting the same perfect alignment that the APD values show down the cable. These results show the prevention of alternans formation all the way down the cable of 150 cells (1.5 cm), as they have identical APDs. The slope of the restitution curve begins to steepen dramatically around a DI interval of 50ms (Figure 13). This can also be observed by the increasing distance between the points between a DI of 100ms until the most left point on the figure corresponding to a DI of 30ms.

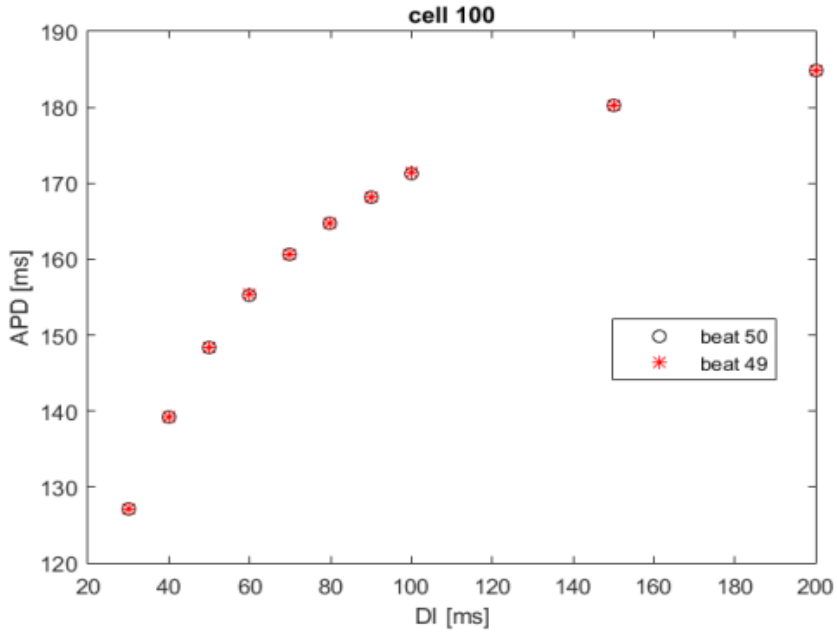

Figure 13 - Shows restitution curve for the 100th cell in the cable, no alternans form throughout the pacing protocol, indicated by the matching of the 49th(red) and 50th(black) stimuli APD values for all DI's tested

3.3 Lengthening cable

To verify that the model prevents alternans in a longer cable model, the number of cells in the cable was increased to 400 cells in the constant BCL model. Figure 14 shows the progression of APD values down the cable (Figure 14). A similar trend for the first 150 cells is seen, that the separation between the long and short beats increases down the cable initially and then slightly shortens toward cell 150. When continuing past cell 150 a node can be observed near cell 200 or roughly 2cm down the cable, when the last odd beat switches from the longer APD to the shorter APD. Similar to previous findings in cables longer than 200 cells, discordant alternans

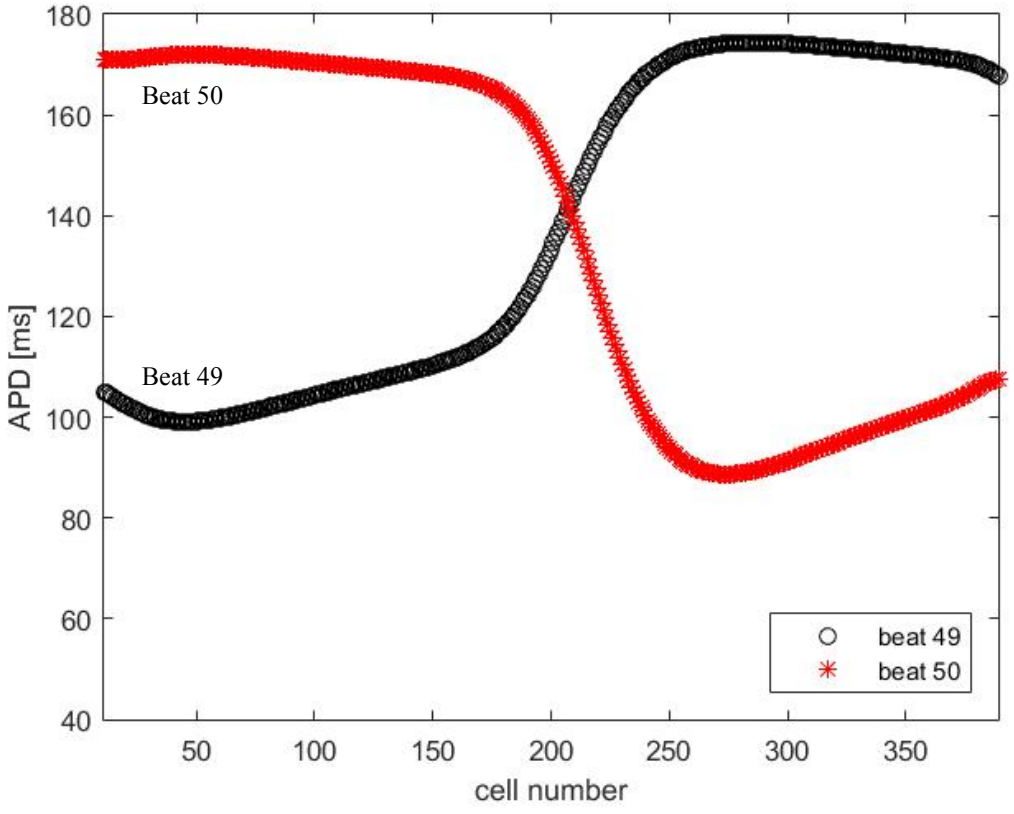

Figure 14 - Constant BCL pacing for 400 cell model paced at 200ms

begin to form (Wei, [18]). Noticeably the lowest APD values after the node corresponding with beat 50, around cell 250, dip below the lowest APD value exhibited by beat 49 before the node seen around cell 50 (Figure 14). Toward the end of the cable it seems as if beat 49's APD values decrease slightly whereas beat 50's values continue the linearly increasing trend seen between cells 300 and 350 (Figure 14).

In contrast Figure 15 shows the APD progression down the cable for the elongated constant DI protocol (Figure 15). A length of 300 cells was chosen because during periodic pacing a node appeared around cell 200, indicating that at this point

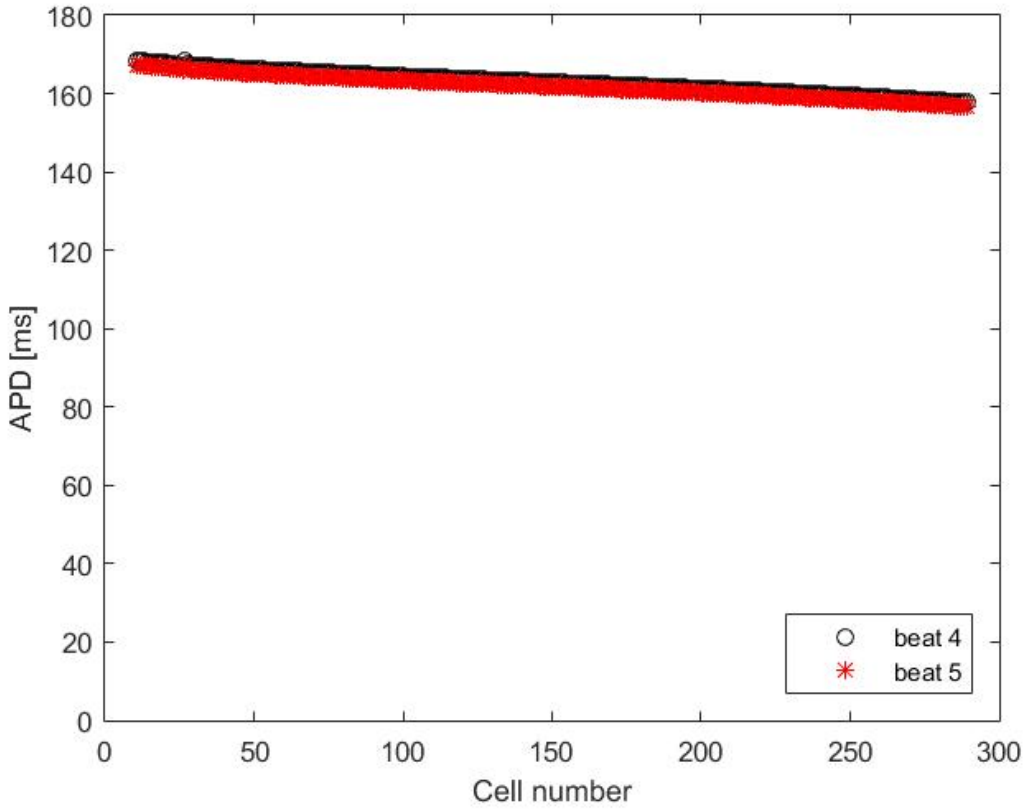

Figure 15 - Constant DI pacing for a 300 cell model at a DI of 55ms

there is ionic instability and if the constant DI pacing would break down it would be at this location (Sato, [34]). Similar trends can be observed in the longer cable as seen in the shorter 150 cell cable. In both the APD values decrease as one proceeds down the cable (Figure 13/Figure 15). The slope decreasing is constant throughout the entire cable with a decrease of .03ms per cell, creating a total drop of 9ms over the entire 280 cells plotted. Once again the first and last ten cells were omitted to eliminate border and stimulation effects.

3.4 Combined protocol

The final test run was to combine the periodic and constant DI protcols to test if altrenans once formed could be prevented. When protocols were switched the associated zoomed in voltage traces can be seen in Figure 16A (Figure 16). At stimuli 20 the switch occurred going from a constant BCL pacing to a constant DI pacing protocol, indicated by the line label constant DI implementation. The transition period lasted for 3 stimuli before alternans were eliminated and the action potentials returned to a uniform shape from beat to beat. Figure 16 shows the correlation between APDs for cell 50 as the various stimuli pass through it creating action potentials, along with the corresponding voltage traces that are associated with the transition from constant BCL to constant DI (Figure 16). At stimuli 20 where the transition is located APD values create a unique pattern of short, long, short, short, for stimuli 17 through 20 (Figure 16B). The trend in Figure 15 is also replicated, meaning that once the constant DI protocol is implemented the APD values slowly starts to decay, forming a slight negative slope as the stimuli continue (Figure 15/16B).

To ensure these findings are valid, a trial was performed increasing the number of stimuli during each protocol. The stimulus number was increased to 50 stimuli for the periodic pacing at 200ms, followed by 50 stimuli at a constant DI of 50ms, to ensure steady state was reached. This trial showed identical results to the shorter stimuli trial, indicating that the combined pacing protocol is robust.

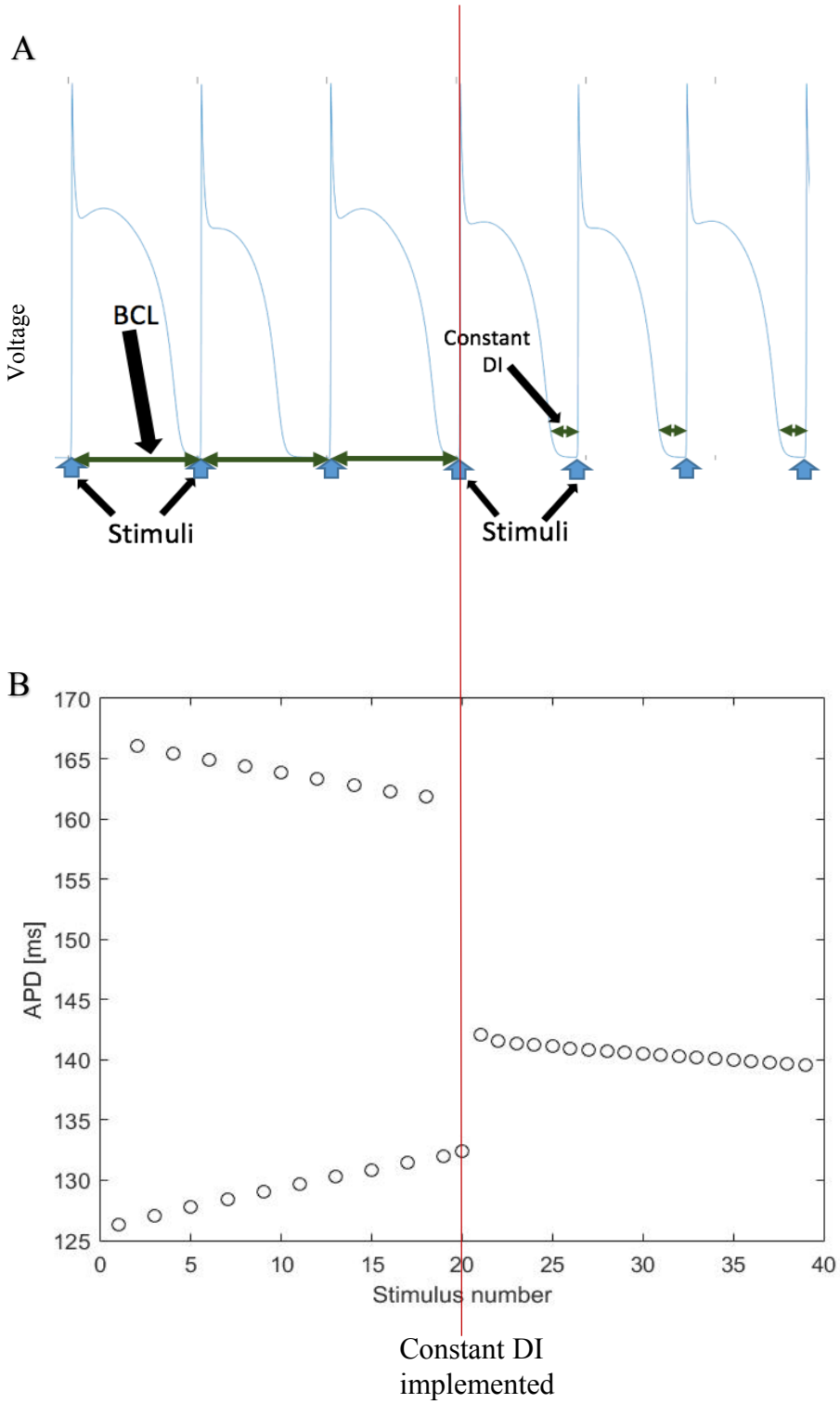

Figure 16 - Cell 50 for combined protocol showing with a constant BCL initially at 200ms followed by a constant DI of 50ms A.) zoomed in version of voltage traces at transition B.) full 40 stimuli plotting all associated APD's

CHAPTER 4

DISCUSSION

4.1 Constant basic cycle length pacing

The constant BCL protocol exhibited alternans formation throughout the cable, seen by the separation of the APD values in Figure 10 by more than 5ms (Figure 10). The increase in spacing between the long and the short beat can be explained by electrical instability created by the formation of alternans. Electrical instability is created by decreasing the pacing cycles intervals. This shortening cuts the action potential's recovery and reset time, therefore the cycle is stopped at different points of repolarization. Eventually, the pacing interval became too rapid. Initially the response transitioned into a 2:1 response followed by a conduction block. 2:1 response is a response pattern during which the second stimulus applied does not trigger an action potential (Fox, [30]).

Electrical instability causes alternans by creating an abnormal distribution of ions across the membrane (Laurita, [31]). Therefore, repetitive identically long action potentials cannot be created, causing abnormally short action potentials to form on intermittent beats in an attempt to compensate in accordance with restitution (Franz, [32]). The changes throughout Figure 10 can be inspected in this light, as the slight increase and decrease between the spacing of the APD values down the cable could be caused by the changing durations of DI leading to electrical instability (Figure 10).

When contrasting Figure 10 to Figure 11 a better understanding of alternans formation and progression can be gained, as Figure 10 shows one instance of the bifurcation graph down the length of the cable. The first relation that can be observed is the instability and its effect on the separation between the two APD values down the cable as well as for each BCL. This inherently showed that periodic pacing creates alternans throughout a short cable that are unstable and dependent on BCL applied as well as location. Along with this observation, it can be deduced that alternans adapt to their environment depending on their distance from the applied stimulus. The causation of this behavior is routed in the preceding DI, as the APD is directly dependent on the time that the membrane was allowed to repolarize. Therefore, from Figure 10 and Figure 11, the time for the DI can be deduced by simply taking the BCL which the cable is exposed to and subtracting the calculated APD (Figure 10/11).

4.2 Constant diastolic interval pacing

Constant DI pacing testing revealed the confirmation of the goal, preventing alternans within a cable model. This can be observed in Figure 12 as both the odd and even beat APDs for the 50^{th} and 49^{th} are almost perfectly superimposed (Figure 12). A slight decline in APD value can be observed as the action potential travels down the cable. This may indicate that as the action potential travels further away from the site of stimulation, the APD shortens as the DI elongates. This would indicate that due to constant DI pacing, the effects of the pacing are seen in the DI as well as the subsequent APD, both of which remain relatively constant (Figure 12). This is in

contrast to the constant BCL pacing model, in which the pacing is more related to the APD accommodating (Franz, [40]).

Similar to Figure 12, Figure 13 shows the alignment of the odd and even beats showing identical values for APD as the DI is decreased (Figure 12/13). This highlights the elimination of the feedback or dependence of APD on the preceding DI. As the dependence has been eliminated by implementing a constant DI pacing, each APD following a fixed DI should have very similar values. This similarity is shown in Figure 13 as the APD points are superimposed and matching for each DI (Figure 13).

Alternans prevention can be seen through the relationship between the APD value for both odd and even beats not changing even with decreasing DI values (Fiugre 13). Due to the limited variation in APD values, between beats it shows that alternans is prevented throughout the cable for all DI values tested. Based on these results we hypothesis that constant DI pacing, by eliminating feedback, is antiarrhythmic and is able to prevent alternans formation within our model.

4.3 Lengthening cable

To confirm that the results of this model were not limited to a 1.5cm cable, as previously shown, the model was extended to 300 cells (3cm). As other groups have shown abilities to control alternans in short cables, the goal of the validation testing was to demonstrate our ability to prevent alternans regardless of length (Jordan, [26]). These tests were done using fewer intervals, and more testing using more stimuli

needs to be conducted to validate these findings. However, initial findings confirm the antiarrhythmic behavior and alternans prevention for constant DI pacing.

Figure 14 shows constant BCL protocol on a 400 cell (4cm) cable (Figure 14). Initially the separation seems to be very similar to the shorter model however around cell 200 a node occurs. A node is when the APD values for the last odd and even beat approach each other and switch their positons. This is known as a spatially discordant alternans (Wei, [18]). Spatially discordant alternans occurs when a cable switches from long APD to short APD during one beat, or vice versa. Node formation is a clear indication of electrical instability and a reason that alternans previously only have been controlled for short cables length around 2.5cm (Kanu, [21]).

Other trends seen in Figure 8 are the variations of slope and shape of the APD graphs following the node. The larger APD before the node, the odd beat, and after the node, the even beat, have a similar shape and slope during steady state. Steady state is defined when no more rapid APD fluctuation occurs, for the odd beat this was between cells 50 and 130. For the even beat steady state was defined between cells 270 and 350.These areas of steady state indicate that the relationship between the long and short APD and their feedback on one another has reached a temporary equilibrium point. This equilibrium cannot hold however, as the corresponding shorter APD has a much steeper slope and never plateaus to a temporary equilibrium point. The slope of the shorter APD appears to increase between the initial even beat to the odd beat right after the node. We hypothesize that the higher slope on the lower APD's post node, indicates that the driving factor behind nodal formation is the desire

of the APD to find a temporary equilibrium that it can only achieve with longer APDs.

The instability of the APD and DI can also be analyzed when looking at the slope close to the pacing location and immediately following the node (Figure 14). The downward slope increases much more after the node has passed, before leveling out at an APD value lower than what was seen for the even beat at the beginning of the cable. It has been shown that after node location conduction block may occur (Wei, [18]). There could be a correlation between the rate of change from APD to APD, for the shorter APD values and this instability causing eventual conduction block as no action potential would be triggered, due to the tissue not being able to recover (Fox, [30]).

Constant DI pacing does prevent alternans even in longer cables and also prevents node formation from occurring. As seen in Figure 15 for the longer cable the APD values along the cable do not line up seamlessly as they did for the shorter cable (Figure 15). This could be caused due to a variety of reasons, the most probable being due to the few number of stimuli applied because of computational time limitations. Based on our previous findings, steady state should have occurred after beat 4. However, as only 5 stimuli were given when comparing beat 4 to beat 5, steady state may not have been reached yet. Further testing needs to be performed to confirm that if more stimuli are applied, the APD values for both the even and odd beat would converge and be superimposed once again. The difference between the odd and even beat APD's in this short proof of concept experiment is only 1ms, and alternans are

defined for this experiment as beat to beat variations greater than 5ms in APD values (Jordan, [26]). Therefore, the change is still well below the threshold and confirming that constant DI prevents alternans even in longer cable models.

4.4 Combined protocol

The next validation testing was the application of both pacing protocols within one cable. By combining the constant BCL and constant DI we investigated if constant DI not only prevents but also suppresses alternans formation within the cable. After twenty stimuli using the constant BCL, the constant DI protocol was implemented.

Transitioning from a alternans prone trace to a alternans free trace indicates that constant DI pacing, by inhibiting the feedback from the previous action potential, does suppress alternans. This can be seen immediately following the implementation of the constant DI protocol, where a unique pattern in APD can be observed. The quick switch and correlation of APD's, also emphasizes that eliminating the feedback immediately suppresses alternans formation.

During the constant BCL pacing of the model the alternans can clearly be identified by large differences in APD values. Similarly, the constant DI can also clearly be seen toward the latter half of the stimulus number. Indicating that constant DI not only has the capability of preventing alternans but can also inhibiting them and taking a rhythm from arrhythmic back to antiarrhythmic. For a better understanding of this process and the effects of varying pacing more research needs to be conducted,

with longer cables as well as more stimuli to completely confirm the findings of this study.

4.5 Clinical significance

Being able to not only prevent but also revert heart rhythm back to normal through constant DI pacing is clinically significant. In the current application of pacing within pacemakers, hearts going into arrhythmic patterns is a true concern, as proarrhythmic pacing can give rise to alternans at certain threshold (Kandaswamy, [33]). Knowing that alternans are precursors to ventricular tachachardia (VT) and ventricular fibrillation (VF), leading to almost certain cardiac death, investigations into the formation, control, and prevention of alternans is a major part of cardiac arrhythmia prevention. In previous studies it has been shown alternans can be controlled in short cables. However our study proposes a pacing protocol, based on feedback elimination, that prevents alternans formation in short as well as long cables (Jordan, [26]). Clinically, this means it could be incorporated into a pacemaker to serve as an antiarrhythmic pacing device. This could most likely cause fewer patients to experience VT or VF through the prevention of alternans, therefore reducing the number of sudden cardiac death's in association with pacemakers.

CHAPTER 5

CONCLUSION

In conclusion, our study set out to find if a previously shown antiarrhythmic pacing protocol, constant DI based on feedback elimination, could be applied to a cable model and also show antiarrhythmic effects throughout the cable. The study demonstrated that constant DI is antiarrhythmic in a cable and that this protocol does not just control alternans but prevents them as well. Constant DI pacing can not only prevent the formation of alternans but also assist in the elimination of alternans that had previously been formed under a periodic pacing protocol. This study has shown that constant DI is a pacing protocol that can control alternans within cables of up to 300 cells (3cm), a result not previously shown.

One limitation of this analysis is the length of cable and the number of stimuli applied. Initial testing was performed but due to computational restrictions, the cable did not exceed 300 cells (3cm) and only five stimuli were applied. Further analysis and testing for an even longer cables and more stimuli needs to be performed, to completely confirm the prevention function found in this study. Another limitation of this study is the use of an older Fox model published in 2002 (Fox, [26]).

By adjusting the Fox model to account for constant DI pacing we have shown that constant DI not only confirms alternans prevention within a single cell, but also within a small and long cable model, and that constant DI has the ability to revert

alternans formation following constant BCL pacing. Therefore, we have confirmed our goal of validating constant DI pacing as being antiarrhythmic within a cable model, as well as a protocol to prevent and eliminate alternans.

REFERENCES

1. Robinson R.B., Siegelbaum S.A. *Hyperpolarization-activated cation currents: from molecules to physiological function.* Annu Rev Physiol 2003;65: 453-480.

2. Vinogradova T.M., Zhou Y., Bogdanov K.Y., Yang D., Kuschel M., Cheng H., Xiao R. *Sinoatrial Node Pacemaker Activity Requires Ca^{2+}/ Calmodulin Dependent Protein Kinase II Activation.* Circ Res 2000;87:760-767.

3. Grant A.O. *Cardiac Ion Channels.* Circ Arrhythmia Electrophysiology 2009;2:185-194.

4. Pinnell J., Turner S., Howell S. *Cardiac muscle physiology.* Cont Educ Crit Care Pain 2007; 7(3): 85-88.

5. Hopkins P.M. *Skeletal muscle physiology.* Contin Educ Anaesth Crit Care Pain 2006; 6(1): 1-6

6. Kolwicz S.C., Purohit S., Tian R. *Cardiac Metabolism and its Interactions With Contraction, Growth, and Survival of Cardiomyocytes.* Circ Res 2013;113: 603-616.

7. Schmidt T.A., Kjeldsen K. *Myocardial K homestasis in ischemia-importance of Na, K-ATPase.* Basic Res in Cardiology 1997; 92(2): 57-59.

8. Barth A.S., Tomaselli G.F. *Cardiac Metabolism and Arrhythmias.* Circ Arrhythmia Electrophysiology 2009; 2: 327-335.

9. Rubart M., Zipes D.P. *Mechanisms of sudden cardiac death.* J Clin Invest. 2005; 115(9): 2305-2315.

10. Jaeger F.J. *Cardiac Arrhythmias.* Cleveland Clinic 2010.

11. Pinski S.L., Fahy G.J. *The Proarrhythmic Potential of Implantable Cardioverter-Defibrillators.* Circ 1995; 92: 1651-1664.

12. Koneru J.N., Swerdlow C.D., Wood M.A., Ellenbogen K.A. *Minimizing Inappropriate or "Unnecessary" Implantable Cardioverter-Defibrillator Shocks* Circ Arrhythmia Electrophysiology 2011;4:778-790.

13. Stevenson W.G., John R.M. *Ventricular Arrhythmias in Patients With Implanted Defibrillators.* Circ 2011; 124: e411-e414.

14. Samie F.H., Jalife J. *Mechanisms underlying ventricular tachycardia and its transition to ventricular fibrillation in the structurally normal heart.* Cardiovascular Res 2001; 50: 242-250.

15. McIntyre S.D., Kakade V., Mori Y., Tolkacheva E.G. *Heart rate variability and alternans formation in the heart: the role of feedback in cardiac dynamics.* JTB 2014; 350(7): 90-97.

16. Rubenstein D.S., Lipsius S.L. *Premature Beats Elicit a Phase Reversal of Mechanoelectrical Alternans in Cat Ventricular Myocytes.* Circ 1995; 91: 201-214.

17. Qu Z., Garfinkel A., Chen P., Weiss J. *Mechanisms of Discordant Alternans and Induction of Reentry in Simulated Cardiac Tissue.* Circ 2000; 102: 1664-1670.

18. Wei N., Mori Y., Tolkacheva E.G. *The role of short term memory and conduction velocity restitution in alternans formation.* JTB 2015; 367 (21): 21-28.

19. Pieske B., Kockskämper J. *Alternans Goes Subcellular: A "Disease" of the Ryanodine Receptor?.* Circ Res 2002; 91: 553-555.

20. Fox J.J., McHarg J.L., Gilmour R.F. Jr. *Ionic mechanism of electrical alternans.* AJP Hear and Circ Phys 2002; 282(2): 516 – 530.

21. Kanu U.B., Iravanian S., Gilmour R.F. Jr, Christini D.J. *Control of action potential duration alternans in canine cardiac ventricular tissue.* IEEE Trans Biomed Eng. 2011; 58(4): 894-904.

22. Wood M.A., Ellenbogen K.A. *Cardiac Pacemakers From the Patient's Perspective.* Circ 2002; 105; 2136-2138.

23. Ramanathan C., Jia P., Ghanem R., Ryu K., Rudy Y. *Activation and repolarization of the normal human heart under complete physiological conditions.* PNAS 2006; 103(16): 6309-6314.

24. Topilski I., Sherez J., Keren G., Copperman I. *Long-term effects of dual-chamber pacing with periodic echocardiographic evaluation of optimal atrioventricular delay in patients with hypertrophic cardiomyopathy >50 years of age.* Am J Cardiol 2006; 97(12): 1769-1775.

25. Kleefeld B., Khaliq A.Q.M., Wade B.A. *An ETD Crank-Nicolson method for reaction-diffusion systems.* Methods Partial Differential Eq. 2012; 28: 1309-1335.

26. Jordan P.N., Christini D.J. *Adaptive Diastolic Interval Control of Cardiac Action Potential Duration Alternans.* J Card Electrophysiology 2004; 15(10): 1177-1185.

27. Wu R., Patwardhan A. *Mechanism of Repolarization Alternans Has Restitution of Action Potential Duration Dependent and Independent Components.* J Card Electrophysiology 2006; 17(1): 87-93.

28. Deo R., Albert C. *Epidemiology and Genetics of Sudden Cardiac Death.* Circ 2012; 125: 620-637.

29. Roger V.L., *Epidemiology of Heart Failure.* Circ Res 2013; 113: 646-659.

30. Fox J.J., Riccio M.L., Hua F., Bodenschatz E., Gilmour R.F. Jr. *Spatiotemporal Transition to Conduction Block in Canine Ventricle.* Circ Res 2002; 90: 289-296.

31. Laurita K.R., Rosenbaum D.S. *Cellular Mechanisms of Arrhythmogenic Cardiac Alternans.* Prog Biophys Mol Biol 2008; 97(2-3): 332-347.

32. Franz M.R. *The electrical restitution curve revisited: steep or flat slope which is better?*. J Cardiovasc Electrophysiol. 2003; 14(10): S140-147.

33. Kandaswamy P.K., Anantha A., Balachander J., Selvaraj R.J. *Heart Failure and Pulsus Alternans: An Unusual Presentation of First-Degree Heart Block.* Circ Heart Failure 2014; 7: 227-228.

34. Sato D., Bers D., Shiferaw Y. *Formation of Spatially Discordant Alternans Due to Fluctuations and Diffusion of Calcium.* PLoS One. 2013; 8(12): e85365

35. Malmivuo J., Plonsey R. *Bioelectromagnetism: Principles and Applications of Bioelectric and Biomagnetic Fields.* New York: Oxford UPU, 1995.